

¹Department of Biotechnology, University of Kotli, Pakistan

²SRL, DHQ Hospital Mirpur, Pakistan

³Department of Botany and Microbiology, College of Science, King Saud University, Riyadh, Saudi Arabia

⁴Department of Botany, Hindu College Moradabad, Mahatma Jyotibaphule Rohilkhand University Bareilly, India

⁵Department of Agronomy, The University of Haripur, Pakistan

Antimycobacterial potential of green synthesized silver nano particles from selected Himalayan flora

Suman Mahmood¹, Sammyia Jannat^{1*}, Asad Hussain Shah¹, Anila Fariq¹, Sajida Rasheed¹, Akhlaaq Wazeer², Saleh H. Salmen³, Mohammad Javed Ansari⁴, Abdul Qayyum^{5*}

(Submitted: January 16, 2024; Accepted: March 2, 2024)

Summary

Mycobacterium tuberculosis (Mtb) is a persistent threat to human life and a challenge to global public health. The pathogen's antibiotic resistance has become a serious problem, prompting the development of nanotechnology-based medicines to prevent multidrug resistance in microorganisms. The present study aimed to synthesize silver nanoparticles (AgNPs), using leaves extracts of *Achillea millefolium*, *Artemisia campestris* and *Hedera nepalensis* to analyze their antimycobacterial potential. The biosynthesized silver nanoparticles were harvested and characterized through UV visible spectroscopy, Field Emission Scanning Electron Microscopy (FESEM) and Energy Dispersive X-ray spectroscopy (EDX). The FESEM analysis showed, that selected plant-based silver nanoparticles were spherical in shape with a diameter ranging from 50 nm to 80 nm. Energy Dispersive X-ray spectroscopy revealed that constitute elements of silver nanoparticles are Ag, C, O, Cl and Ca. The biosynthesized AgNPs exhibited significant antibacterial potential against *Mycobacterium tuberculosis*. At a concentration of 50 µL *Hedera nepalensis* exhibited the highest growth inhibition at 97.33%, followed by *Artemisia* at 95%, whereas the percentage growth inhibition of *Achillea millefolium* at 50 µL concentration was 72.33% as compared to the Rifampicin (RIF) i.e., 40%. Fluorescence microscopy confirmed visible growth inhibition in both experimental and controlled cultures. *Hedra nepalensis* and *Artemisia campestris* showed promising potential to inhibit the growth of mycobacteria populations, indicating their potential for the development of novel nanomedicine to treat tuberculosis effectively.

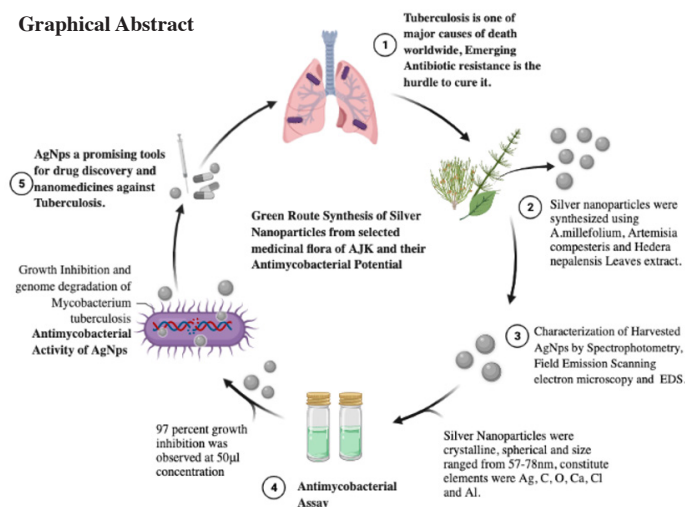
Key words: Tuberculosis; medicinal plants; silver nanoparticles; anti-mycobacterial potential.

Introduction

Tuberculosis (TB) is a contagious disease that is a leading cause of illness and mortality. It is caused by airborne *Mycobacterium tuberculosis*. It can manifest as both pulmonary and extra-pulmonary forms, though the global population exhibits a higher ratio of pulmonary tuberculosis cases. In 2020, TB caused the death of 1.5 million people. Worldwide, TB is the thirteenth main reason of death and the second most deadly disease after COVID-19 (NATARAJAN et al., 2020). In 2020, an estimated 10 million people contracted TB worldwide, including 5.6 million men, 3.0 million women and 1.1 million (WORLD HEALTH ORGANIZATION Global Tuberculosis, 2020). Eight nations, namely India, Indonesia, China, Philippines, Pakistan, Nigeria, Bangladesh, and South Africa, accounted for two-thirds of the new TB cases, according to the World Health Organization's data from 2019 to 2020. In Pakistan, TB is a prevalent infectious disease

* Corresponding authors

Graphical Abstract



that widely affects the population in rural and underdeveloped regions. Patients with active pulmonary TB are the primary source of contamination, and the majority of people infected with *M. tuberculosis* have asymptomatic latent TB infections (LTBI) (TAHSEEN et al., 2020). It is estimated that approximately 2 billion individuals worldwide harbor latent tuberculosis infection (LTBI), rendering them susceptible to the potential reactivation of the disease (DYE et al., 1999; DIEL et al., 2013).

There is a persistent need for improvement and greater green assessment of the latest TB tablets and shorter remedy regimens. No new TB drug instructions have been developed or authorized for drug-prone TB since the introduction of the modern-day 6-month four-drug combination the 1970s. The lack of coordinated drug improvement and new combinations has led to the introduction of fixed-dose combinations of two (isoniazid and rifampicin), three (isoniazid, rifampicin, and pyrazinamide) and four (isoniazid, rifampicin, pyrazinamide, and ethambutol) tablets (LIENHARDT et al., 2011; HUANG et al., 2023). Plant-based drugs have been used historically for disease control, but their extensive use has substantially increased in the last decade. By the end of 20th century, 170 natural medicines have gained reputable recognition. Medicinal plants are a reliable and an indispensable source of natural bioactive compounds. According to WHO, approximately 80% of the world's population is still relies on the use of medicinal plants for their primary healthcare and for the development of a myriad of medicines (HAQ et al., 2004; WHO, 2022). Currently, more than 40% of pharmaceutical formulations are derived from natural ingredients. These include commercially available medicines such as digoxin, chloroquine quinine, lumefantrine, atovaquone, aspirin and artemisinin (WOODLEY et al., 2021; WHAYNE et al., 2018).

Azad Jammu and Kashmir (33°45'16"N 73°56'38"E) have a diverse range of plants with significant medicinal properties. With the growing concern for human health, the significance and utilization of medicinal plants are extended due to their clean availability, lesser side effects and less cost. There is a need to explore the potential of natural medicines compared as alternative to synthetic drugs.

Achillea millefolium, also known as yarrow or common yarrow, is a flowering plant belonging to the Asteraceae family. It is distributed in temperate areas of the Northern Hemisphere in Asia, Europe, and North America. The plant typically grows from May to July. *Achillea millefolium* leaves are used as treatment to remedy TB, belly pain, and fever. It is reported to be utilized on jaundice, hepatitis, typhoid, fever, and tuberculosis disorders (AHMAD et al., 2017).

Artemisia campestris, commonly known as wormwood, is an extensive species of the sunflower family, Asteraceae. It is widely distributed in Eurasia and North America. *Artemisia campestris* extracts have a significant capacity for remedy of tuberculosis infections, and it also contain bactericidal compounds (MARTINI et al., 2020).

Hedera nepalensis (Himalayan ivy, chang chun teng) is a perennial plant that belongs to the genus *Hedera*. It is native Nepal and Bhutan, as well as Afghanistan, Pakistan, India, China, Laos, Myanmar, Thailand, and Vietnam, at altitudes of approximately 1000-3000 m. Plants can reach heights of 30 m, with easy leaves starting from 2-15 cm long, and yellow vegetation. *Hedera nepalensis* is notably utilized in conventional Chinese remedy to deal with rheumatism by enhancing blood circulation, decreasing congestion, and assuaging pain (HE JING, 1978). The *Hedera* Linn. plant extract contains numerous secondary metabolites with anticancer, anti-diabetic, and antioxidant properties (SALEEM et al., 2014; HE et al., 2023; XIA et al., 2023).

The versatility of plant-based metallic nanoparticles makes them some of the most promising diagnostic and therapeutic entities in modern medicine. Recently, there has been significant increase in the biosynthesis of metallic nanoparticles (MNPs) from medicinal plants that are essential in the development of theragnostic (XULU et al., 2022). The use of plant-based nanoparticles attracted the attention of researchers due to their cost-effectiveness, rapidity, and safety (KOWSHIK et al., 2003). In the field of drug delivery, nanoparticles (NPs) with antimicrobial properties have garnered significant attention for their potent bactericidal effects and resistance to metallic ions. (KUMAR and ANTHONY, 2016). Nanoparticles of 1 to 10 nanometer in size connect to the outer overlaying of molecules, significantly reducing permeability of membrane and cellular respiration pathways. Nanoparticles are furthermore successful in infiltrating microbes as a result imposes greater incorporation in the DNA resulting in degradation (RAMAR et al., 2015). Particularly in the discipline of health science and therapeutics, silver nanoparticles are reported with great potential. Silver is a robust anti-microbial agent and dangerous to dwelling cells. Silver has the capacity to disrupt molecular walls of microbes, preventing microbial growth and interrupting molecular mechanisms because of their ability to interact with large molecules within the cells (DNA and proteins) (VAZQUEZ-MUÑOZ et al., 2017). The synthesis of nanomedicines targeting *Mycobacterium tuberculosis* holds promise in combating the deadly disease of tuberculosis and reducing cases of multiple drug resistance in patients. The present study aims to synthesize silver nanoparticles from selected medicinal flora of Azad Jammu and Kashmir, characterize them using advanced techniques and evaluate their antimycobacterial potential for treating tuberculosis.

Materials and methods

Collection of plant sample

For the green synthesis of silver nanoparticles (AgNPs) from plant material, the plant species *Achillea millefolium*, *Artemisia campestris*

and *Hedera nepalensis* were collected from forests of Azad Jammu and Kashmir (33°29'59"N 73°52'51"E).

Preparation of plant extract

Leaves and stems were shade-dried and crushed into a fine powder. The powdered material was dissolved in autoclaved distilled water at a ratio of 1:10 (10 g solute/ 100 mL solvent). The solution was put on the shaker for 48 h for constant stirring and shaking. This thoroughly dispersed the plant material within the water. After 48 h, each crude extract (*Achillea millefolium*, *Artemisia campestris* and *Hedera nepalensis*) was filtered thrice, once with the gauze strainer and twice with Wattman No 1 Filter paper until no suspended particle was seen in the obtained extract. The obtained extract was then further purified by using a Rotary Evaporator apparatus. The extra water was evaporated by adjusting the temperature to 90 °C for 45-50 min until a pure viscous extract was obtained, which was stored in falcon tubes for later use at room temperature.

Green synthesis of Silver Nanoparticles

Preparation of 2.5 mM silver nitrate stock solution

For the synthesis of AgNPs, the 2.5 mM stock solution of silver nitrate was prepared as follows: for each 2.5 mM solution 0.4246 g silver nitrate salt (Sigma Aldrich, Germany) was dissolved in 1000 mL autoclaved distilled water, stored in ambered bottle in dark place for 24 h. After 24 h, the stock is ready to use for further synthesis of nanoparticles from the prepared extract (PIRTARIGHAT et al., 2019).

Green synthesis of AgNPs from plant extracts

The reaction for the green nanoparticles synthesis is set by dissolving 5 mL of plant extract into 45 mL of 2.5 mM silver nitrate solution, in a tinted covered falcon tube to avoid any exposure to the light. The pH of the solution is adjusted to 12 by adding NaOH. The color change due to oxidation was observed. The containers were kept in dark for 24 h, after that the suspended AgNPs were ready for extraction (GHAFFARI-MOGHADDAM et al., 2014).

Extraction of silver nanoparticles

After 24 h the suspended nanoparticles are collected via centrifugation for 10 min at 12000-14000 rpm. The supernatant is discarded, and pellet was rinsed with distilled water again centrifuged and dried in a dry oven. After drying the pellet is crushed into fine powder for further assay and stored in dark containers at room temperature (GHAFFARI-MOGHADDAM et al., 2014).

Characterization of silver nanoparticles

The synthesized silver nanoparticles were characterized by Spectrophotometry, Field Emission Scanning Electron Microscope (FESEM), Energy Dispersive Spectroscopy (EDS) and Fourier transform infrared spectroscopy (FTIR).

Spectrophotometric analysis for full spectra reading

After 24 h of the reaction of plant extract with 2.5 mM silver nitrate, the samples were observed for the synthesis of suspended nanoparticles, for full spectra reading and the spectrophotometric analysis was performed at wavelength 300-800 nm. Using 2.5 mM silver nitrate stock solution as reference, the optical density (OD) and maximum peaks in the range was observed at 1X, 2X and 3X distilled water dilution of silver nitrate with plant extract (SASTRY et al., 1997).

Field emission scanning electron microscope (FESEM) characterization

For SEM analysis the fine crushed dried nanoparticle material was prepared by subjecting to sputtering. The sputter coating of the samples was done before working with SEMs to obtain high quality images. The sputter coating of silver nanoparticles was done by using SAFEMATIC compact coating unit CCU-010 at pressure 5.0e-2mbar with Au-Pd 60/40 as coating material. After the sputter coating, the samples were subjected to beam of electrons and the images were obtained at different resolutions which revealed the shape, size, and structure of silver nanoparticles (JAGTAP et al., 2013).

Energy dispersive Spectroscopy (EDS)

Energy Dispersive spectroscopy was done along with the FESEM, MIRA3 TESCAN has Oxford EDS detector. Each nanoparticle sample was subjected to EDS detector to obtain the elemental content and composition (JAGTAP et al., 2013).

Fourier Transform Infrared (FTIR) Characterization

For FTIR spectroscopic analysis, sample was prepared by grinding 1 mg of dried biosurfactant with 100 mg of KBr and pressed at 7500 kg pressure with hydraulic press to acquire transparent pellet. Pellets for nanoparticles were made by the same procedure and analyzed with FTIR spectrometer at the range of 500-4000 cm^{-1} with the resolution of 4 cm^{-1} (FARIQ and YASMIN, 2020).

Antimycobacterial Assay

Preparation of AgNPs stock solution

The 100 mg stock solution was prepared by suspended 100 mg Silver Nanoparticles in 10 mL of autoclaved distilled water. The stock is stored in dark and used for antimycobacterial activities (SRIKAR et al., 2016).

Preparation of Bacterial Media

For 1200 mL of Lowenstein-Jensen (LJ) media, 2.7 g L asparagine, 1.8 g potassium di hydrogen phosphate, 0.45 g magnesium citrate, 0.18 g magnesium sulphate are mixed well with 450 mL of distilled water and 9 mL glycerol on a magnetic stirrer and autoclaved. 0.3 g malachite green was dissolved in 15 mL distilled water and mixed with 750 mL of egg homogenate with the help of beads shaker. The autoclaved salt solution, malachite green and egg homogenate are mixed well, and 5-6 mL of media is poured into universal media tube bottles. After pouring of media, the media tubes are cooked on 85 °C for 2 h on slop oven, to create slope for the growth to be visible. After 2 h the media is fully cooked and placed in incubator for sterility test. After 24 h of sterility test, the visible color change or growth was not observed. The LJ media was ready to use for further cultures and sub culturing (KASSAZA et al., 2014).

Antimycobacterial Activity

The inoculum of *Mycobacterium tuberculosis* was obtained from State reference Tuberculosis laboratory (SRL), National TB control Program (NTP), Mirpur Azad Kashmir, 10250 Pakistan. One loop full of the bacterial load was picked with the help of inoculating loop under Biosafety cabinet, ensuring all personal protection of BSL-3 and suspended in 5 mL of autoclaved distilled water and mixed properly through vortex mixer.

From the inoculum, 50 μL was picked using micropipette and the labelled universal culture tubes containing 5 mL media were inoculated drop by drop. After the inoculation, AgNPs solution for each plant was inoculated only in experimental tubes with the 50 μL concentra-

tion. The lids were closed and placed in the incubator for 2–3 weeks at 37 °C. After the required growth time period of MTB, the optical density was measured. The procedure was repeated for 40 μL , 30 μL , 20 μL concentrations of silver nanoparticles for the percentage growth inhibition activity of silver nanoparticles at different concentrations (SRIKAR et al., 2016).

Measurement of Optical Density

Growth inhibition in percentage of pathogenic strains was calculated by measuring absorbance values at 600 nm in Spectrophotometer.

$$\text{Percentage of inhibition of growth} = (\text{A}_p - \text{A}_n / \text{A}_p) \times 100$$

Whereas

A_p = Absorbance of pathogenic strain, and

A_n = Absorbance of strain + nanoparticles.

For this loop full of strain colonies obtained from each culture were suspended in 5 mL of 70 percent ethanol to ensure the safe transfer of pathogen outside of biosafety cabinet (SRIKAR et al., 2016).

Fluorescence Smear Microscopy for Acid Fast Bacilli (AFB)

For fluorescent microscopy, the slides were stained with auramine. The smear of droplet of culture was made on glass slides, which were heat fixed. After heating, auramine dye was poured over the slides and kept for 20 min. After 20 min, the slides were rinsed with water and acid alcohol was poured for 2 min, rinsed and the counter stain methylene blue was poured for one minute. After that the slides were rinsed with water, dried, and examined.

Auramine staining was done on smear slides prepared from both control and experimental culture inoculum and observed under 40 \times and 100 \times lenses of fluorescence microscope to observe morphology of MTB colonies (MAY et al., 2019).

Subculture for Cell Viability

After 2-3 weeks of the culture for antimycobacterial assay, the loopful of colonies (if any) were picked from both control and experimen-

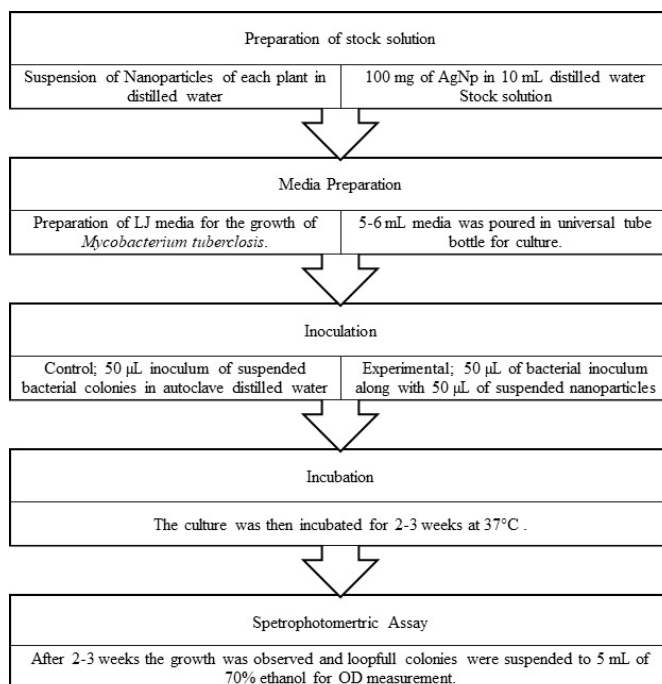


Fig. 1: Generalized pathway for different assays performed for antimycobacterial properties of AgNPs.

tal cultures and subculture to observe cell viability for 2-3 weeks. After which the visible growth will confirm that the inoculum cells were viable or not (SRIKAR et al., 2016).

Statistical Analysis

All data was presented as the mean value of three independent replicates \pm the standard error (SE). Statistical study was carried out by Completely Randomized One-Way Analysis of Variance (ANOVA) test using Statistix Software, version 10 at a 1 percent significance level ($P < 0.01$) (FRAIMAN and FRAIMAN, 2018).

Results

In the present study silver nano particles of *Achillea millefolium*, *Artemisia campestris* and *Hedera nepalensis* were synthesized and characterized.

Physical Appearance

The initial color of the reaction mixture of 2.5 mM Silver Nitrate with plant extract showed a pale-yellow color, after 24 h oxidation and formation of oxides, the color changed to dark brown (Fig. 2).

Ultraviolet Visible Spectroscopy

The biosynthesis of AgNPs was detected by measuring the absorbance within the range of 300-700 nm, at different pH and temperature conditions. Two sharp peaks appeared at 445 nm and around 465 nm of UV visible spectrum that showed the AgNPs biosynthesis and this range was reported as “surface Plasmon resonance band” of biosynthesized AgNPs (Fig. 3).

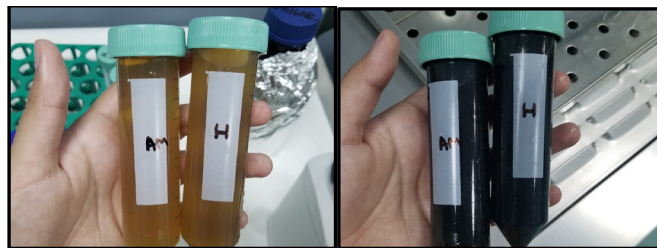


Fig. 2: The color change can be observed after the reaction between the plant extracts and silver nitrate at pH 11-12 due to oxidation and formation of suspended Silver Nanoparticles.

Field Emission Scanning Electron Microscope (FESEM)

SEM was performed to determine size and surface morphology of silver nanoparticles. The silver nanoparticles of *Achillea millefolium* were found spherical between size of 50 nm to 80 nm. FESEM image of round, circular shaped silver nanoparticles of *Artemisia campestris* is showing the size of 63-68 nm (Fig. 4).

Energy Dispersion X-ray Spectroscopy (EDS) Analysis

Through Energy Dispersion X-ray Spectroscopy, the crystalline nature of silver nanoparticles was determined. The nano-crystals of silver exhibited a classical optical peak of absorption at 3 keV owing to Surface Plasmon Resonance (SPR). The maximum absorption peak at 3 keV depicted that these biosynthesized NPs were mostly comprised of Ag which displayed crystalline nature. It can be observed that the silver content was high in the silver nanoparticles along with the presence of chlorine, oxygen and aluminum, calcium. The higher content of silver suggests the production of silver nanoparticles. The capping agents are plant materials (Fig. 5).

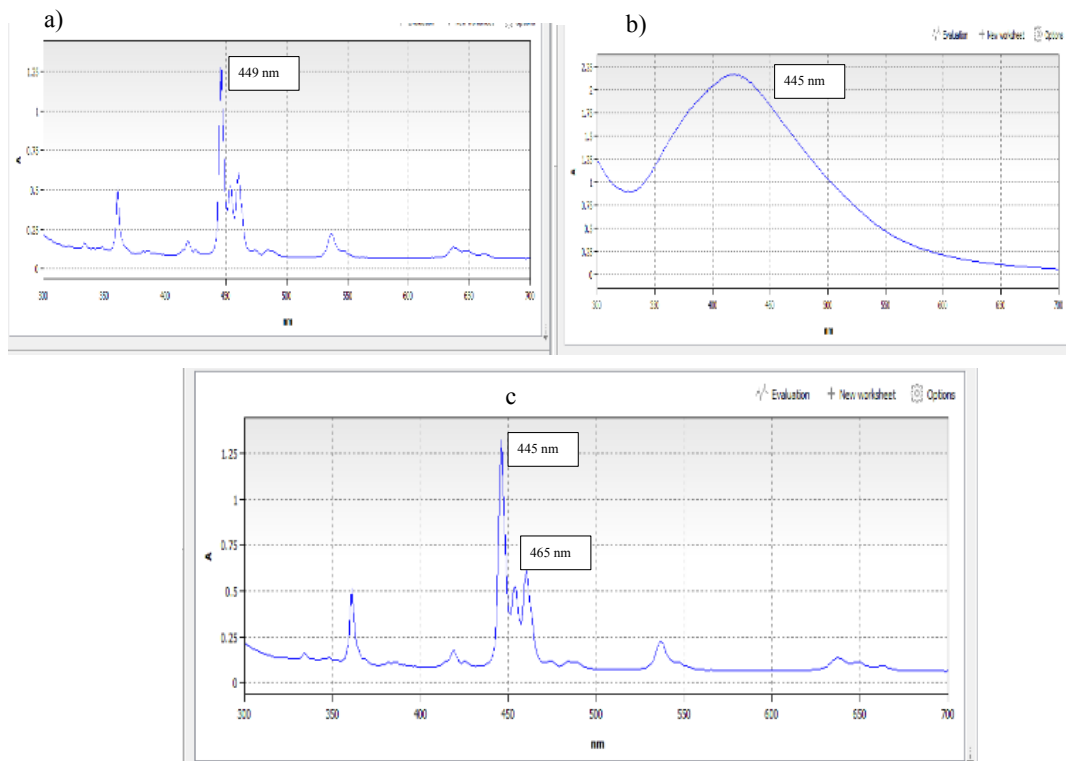


Fig. 3: 2.5 mM silver nitrate stock solution as reference, the OD and maximum peaks in the range of 300-800 nm were observed. Two sharp peaks appeared at 445 nm 449 nm and around 465 nm of UV Visible spectrum confirming the synthesis of suspended AgNPs of (a) *Achillea millefolium*, (b) *Artemisia campestris*, (c) *Hedera nepalensis*.

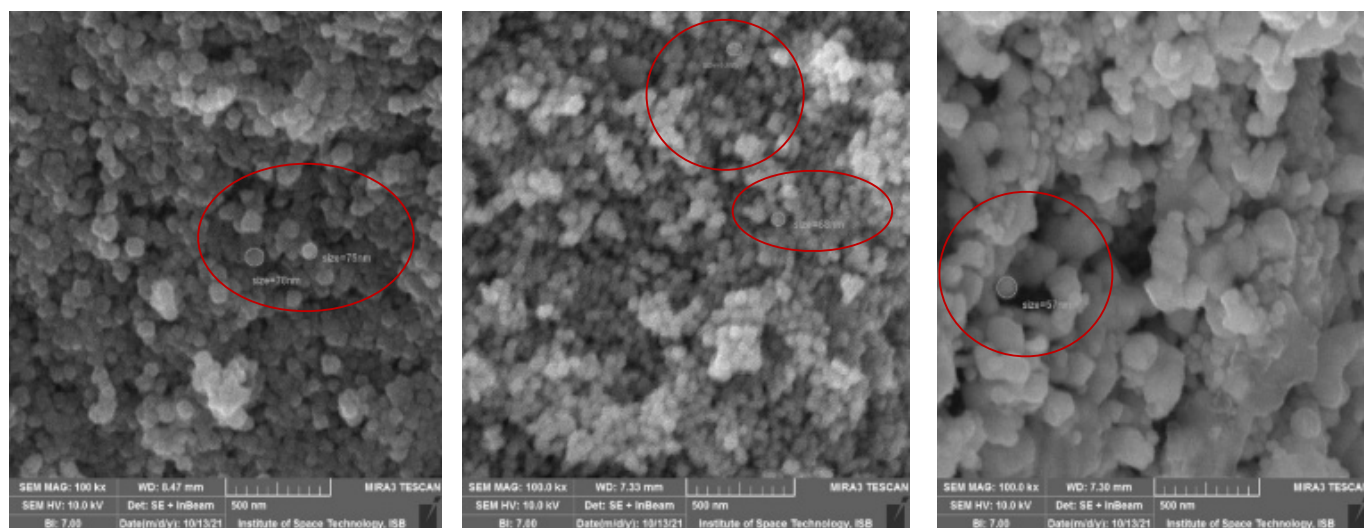


Fig. 4: (Left to right) FESEM image of silver nano particles of *A. millefolium* showing size of nanoparticles between the range of 75-78 nm, *Artemisia campestris* showing the size of 63-68 nm, *Hedera nepalensis* of size 57 nm.

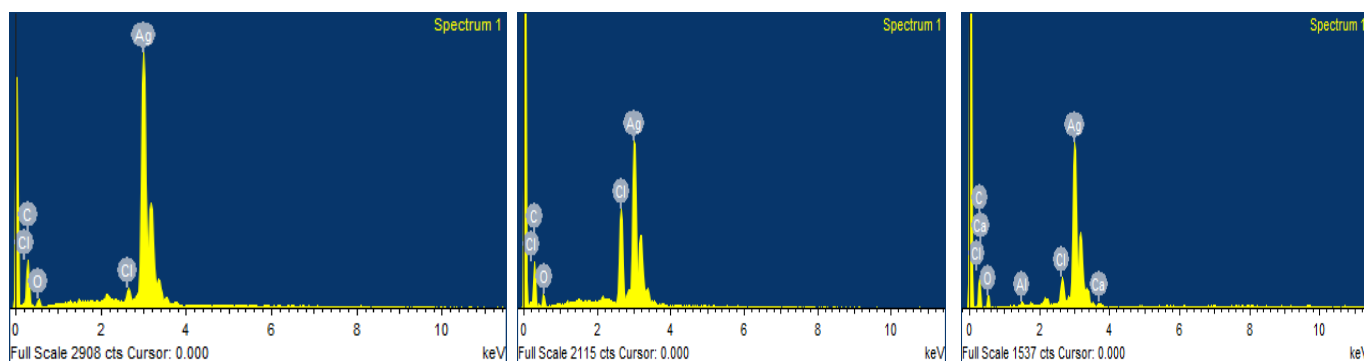


Fig. 5: (Left to right) EDX image of silver nano particles of *A. millefolium*, *Artemisia campestris* *Hedera nepalensis*. The major element found is Ag confirming the Silver Nanoparticles, other constitute elements are C, O, Ca, Cl and Al respectively.

Fourier Transform Infrared (FTIR) Characterization

Various functional groups of the biomolecules were observed from the analysis. In case of *Achillea millefolium* silver nanoparticles, the IR peaks at 2951.19 refers and corresponds to -CH₃ functional group, IR peak at 1614.47, 829.42 and 1454.38 corresponds to aromatic compounds of the functional groups which could be terpenes and carotenoids (Fig. 6). Similarly, the peak at 1217.12 corresponds to alcoholic functional group. In case of *Hedera nepalensis* silver nanoparticles, IR peak at 3425.69 corresponds to -OH group of phenols. The IR peak at 2087.05 corresponds to aromatics functional groups of terpenes likewise, IR peak at 1643.41 also corresponds to phenolics and flavonoids group of plant metabolites (Fig. 6). In case of *Artemisia campestris* silver nanoparticles, the IR peak at 2997.43, 2397.60 corresponds to alkanes functional groups, 1614.47, 14158.30 corresponds to aromatics such as artemisinin a terpene presents in *Artemisia campestris*. The IR peak at 1084.74 corresponds to -OH group referring to alcohols (Fig. 5).

Antimycobacterial Activities

The percentage growth inhibition was observed for each silver nanoparticle suspension at different concentration. For negative control, a subculture of *Mycobacterium tuberculosis* was used. For positive control Rifampicin, which is the WHO standard treatment for *Tuberculosis*. The percentage growth inhibition of Rifampicin

(RIF) at 50 μ L is 40.00 \pm 0.58. For the concentration of 30 μ L of silver nanoparticles suspension the percentage growth inhibition of *Artemisia campestris* is 33.00 \pm 0.58. The growth inhibition percentage of *Achillea millefolium* at 30 μ L concentration was 69.00 \pm 0.58 and the inhibition of *Hedera nepalensis* was 47.67 \pm 0.33.

The concentration of 40 μ L of silver nanoparticles suspension was used for the percentage growth inhibition of MTB culture. For the concentration of 40 μ L of silver nanoparticles suspension, the percentage growth inhibition of *Artemisia campestris* is 36.00 \pm 0.577. The percentage growth inhibition of *Achillea millefolium* at 40 μ L concentration is 54.00 \pm 1.155 and the inhibition of *Hedera nepalensis* is 46.67 \pm 0.882. The concentration of 50 μ L of silver nanoparticles suspension was used for the percentage growth inhibition of MTB culture. For the concentration of 50 μ L of silver nanoparticles suspension, the percentage growth inhibition of *Artemisia campestris* was 95.00 \pm 0.577. The growth inhibition of *Achillea millefolium* at 50 μ L concentration was estimated 72.33% \pm 0.333 and the inhibition of *Hedera nepalensis* was observed 97.33% \pm 0.33 (Fig. 7). The maximum growth inhibition was observed at 50 μ L concentration, in case of *Hedera nepalensis* denoted by H the maximum value of 97.33 was observed. *Artemisia campestris* (A) showed the growth inhibition of 95. The percentage growth inhibition of Rifampicin (RIF) was 40.00 \pm 0.58.

Analysis of Variance (ANOVA) was employed to find the variation of different concentrations biosynthesized silver nanoparticle suspen-

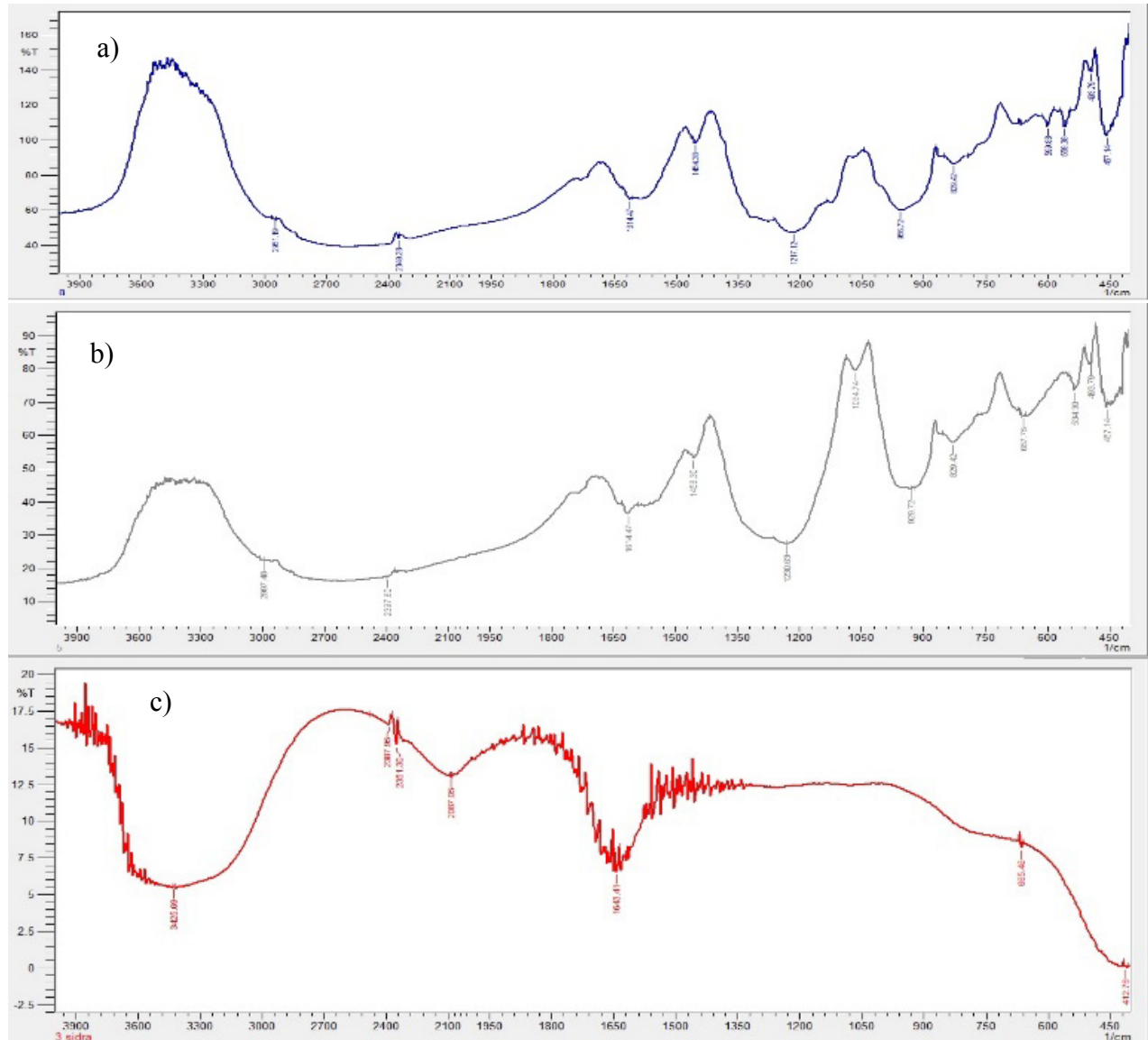


Fig. 6: The FTIR results of a) *Achillea millefolium* b) *Artemisia campestris* c) *Hedera nepalensis*.

sions to inhibit growth of *Mycobacterium tuberculosis* strain. Their grand mean values and critical values ranged from 54.667 to 67.111 and 1.67 to 15.33 respectively while the P values of *Hedera nepalensis* and *Achillea millefolium* silver nanoparticle suspensions were equal to 0.00 as indicated in Tab. 1 which depicted the highly significant variation ($P=0.001$) among different concentration of biosynthesized AgNPs to which MTB strains were exposed.

Tab. 1: Analysis of Variance (ANOVA) showed variation for inhibition of *Mycobacterium* strain using different concentrations of silver nanoparticle suspensions.

Silver Nanoparticles	MSE	MS con	GM	CV
<i>Achillea millefolium</i>	0.83	3667.00**	54.667	1.67
<i>Artemisia campestris</i>	105.778	638.778	67.111	15.33
<i>Hedera nepalensis</i>	0.78	2517.44**	63.889	1.38

*Shows significant variation based on the p value, **shows highly significant variation based on the p value.

Cell Viability Assay

The subcultures of previously treated strains with silver nanoparticle suspensions showed no progress in growth of the colonies of *Mycobacterium tuberculosis* after 3 weeks of inoculation and incubation at 37 °C. This confirmed the antimycobacterial activities of silver nanoparticles synthesized by different plants in current study.

Fluorescence Microscopy

The fluorescence microscopy was used to visualize the bacterial load on both the control and experimental cultures and the morphology of the bacterium after the application of silver nanoparticles. The bacterial load was visibly lower in the slides observed, after the application of silver nanoparticles on the culture (Fig. 8). The proposed mechanism of action of AgNPs on AFB (RAMAR et al., 2015) is shown in Fig. 9.

Discussions

Bio-nanotechnology has emerged as connection between nanotechnology and biotechnology for producing biosynthetic and environmentally friendly technology for production of nanomaterials. Silver

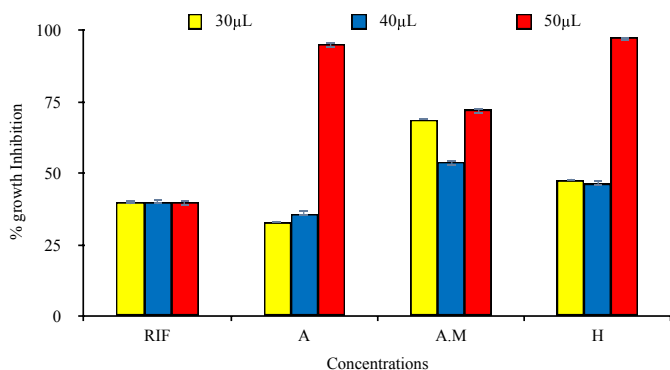


Fig. 7: Percentage growth inhibition of silver nanoparticles against *Mycobacterium tuberculosis*.

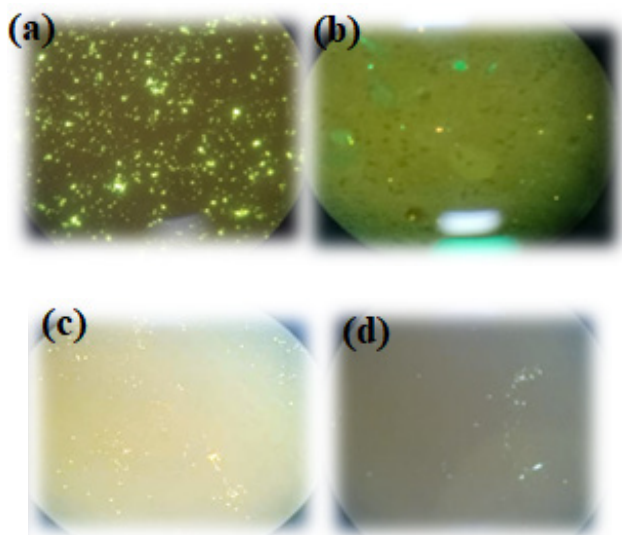


Fig. 8: (a) Auramine staining fluorescence micrograph of control culture smear, (b, c, d) micrograph of culture smear treated by silver nanoparticles of *Achillea millefolium*, *Artemisia campestris* *Hedera nepalensis*.

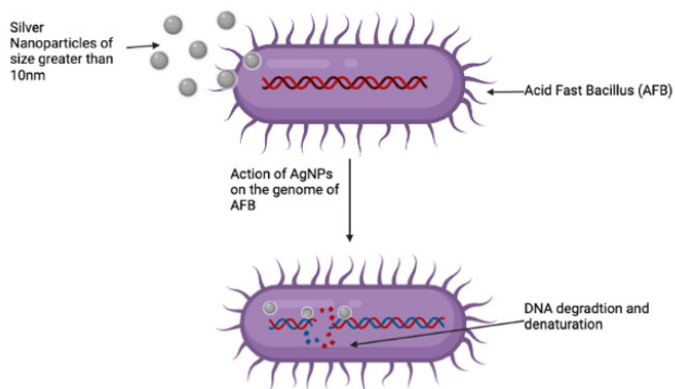


Fig. 9: Proposed mechanism of action of AgNPs on AFB (RAMAR et al., 2015).

has long been known for its strong antibacterial potential. The dimensions of nanoparticles are much smaller as compared to that of most natural structures; hence, nanoparticles might be beneficial for both *in vitro* and *in vivo* biomedical research field. The synthesis of AgNPs increased greatly with increasing temperature and in alkaline

conditions. The rate of synthesis was almost non-existent in acidic conditions, and was found to be maximum at pH 13. These results are consistent with those documented by (KREDY, 2018) where an increase in AgNPs synthesis was observed with increasing temperature and alkaline conditions. ALVES et al. (2022) examined the combined effects of pH, time, and temperature on AgNPs mycosynthesis and found that higher temperatures (90 °C) and basic pH (9 and 12) were more favorable for the synthesis of smaller, monodisperse AgNPs. The role of AgNPs in bactericidal process is unexplained till now, although several mediated hypotheses are exploitable in previous studies. It could be argued that AgNPs have the potential to adhere and penetrate the cell wall of the strain. The configuration of small holes in the cell membrane of bacteria causes the escape of cytoplasmic liquid from cell membrane ultimately cell life gets compromised (AHMAD et al., 2020; XIANG et al., 2023; LI et al., 2019). Another possible reason is the release of ions from NPs which can suppress the activities of catalysts responsible for respiration and disrupts respiratory series, ultimately generating reactive oxygen species. These Reactive oxygen species might cause oxidation pressure to the strain and, as a result, all activities stop ultimately resulting in cell death (RAMAR et al., 2015; YI et al., 2018). Our results demonstrate that the silver nanoparticles of selected plants showed peaks associated with the different compounds or metabolites with potential medicinal properties. Furthermore, the nature of interaction between microorganisms and metal atoms can be exposed by understanding the structural changes in the molecular binding.

Our findings showcased that bio-synthesized AgNPs showed significant anti-mycobacterial activities against tuberculosis-causing bacteria. Silver nanoparticles are a promising solution to this problem due to their broad-spectrum antimicrobial properties (TANG et al., 2018; YI et al., 2023). ROY et al. (2019) studied anti-bacterial properties of *Euphorbia acruensis* synthesized AgNPs concluding that plant latex had no concern with anti-bacterial action, but the AgNPs synthesized from latex exhibited maximum bactericidal potential with increase in AgNPs concentration. AgNPs have reportedly been proposed as novel antimicrobial agents with anti-bacterial, anti-biofilm, anti-fungal, and anti-viral properties. AgNPs' potent antibacterial action makes them effective against germs that are resistant to multiple drugs (MDR) (TUFAIL and LIAQAT, 2021). Our results showed significance of silver nanoparticles synthesized by the green route, the silver nanoparticles synthesized by selected flora found to possess anti mycobacterial properties.

At 50 μL the maximum growth inhibition was observed by *Hedera nepalensis* up to 97.33% and *Artemisia campestris* showed the growth inhibition of 95%. The growth inhibition of *Achillea millefolium* at 50 μL concentration has been estimated up to 72.33% as compared to the Rifampicin (RIF) with 40%. The minimum percentage growth inhibition was observed at 30 μL by *Artemisia campestris* was 33%. The results for *Hedera nepalensis* and *Achillea millefolium* were highly significant p value $P < 0.01$. Both *Hedera nepalensis* and *Achillea millefolium* have shown promising results against mycobacteria when compared to commonly used synthetic drugs against tuberculosis. The percentage of growth inhibition was directly proportional to the concentration of silver nanoparticles. The conclusions of ROY et al. (2019) displayed high agreement with our results where there is an increase in bactericidal potential with increasing concentration of AgNPs. BEZZA et al. (2020) also displayed high agreement with our findings that AgNPs have strong antibacterial activity and may be used to treat bacteria that are resistant to many drugs by acting indiscriminately on the lipopolysaccharide layer of Gram-negative and the peptidoglycan layer of Gram-positive bacteria. The visible growth inhibition was confirmed by Fluoresce microscopy.

These biosynthesized AgNPs hold promising potential in the synthesis of nano-medicine against tuberculosis. Nanoparticles smaller than 10 nm combine with bacteria to induce electrical effects that

increase the reactivity of the nanoparticles. Consequently, it has been confirmed that the size-dependent bactericidal activity of silver nanoparticles exists (RAI et al., 2007). The geometry of the nanoparticles also affects their antibacterial activity, as demonstrated by research on how differently shaped nanoparticles limit bacterial growth. PAL et al. (2007) reported that truncated triangular nanoparticles containing 1 µg of silver exhibit bacterial suppression. On the other hand, 12.5 µg of total silver content is required for spherical nanoparticles. The rod-shaped particles require a total silver concentration of 50–100 µg. Therefore, the impacts of variously shaped silver nanoparticles on bacterial cells are distinct.

Conclusions

The anti-mycobacterial properties of synthesized silver nanoparticles from *Hedera nepalensis* and *Artemisia campestris* were estimated against the mycobacteria respectively. Both the plants exhibited strong anti-mycobacterial properties even at using 50 µL quantity showed growth inhibition. The growth inhibition of MTB culture increased with the concentration of silver nanoparticle suspension. The results may be valuable in the synthesis of nano-medicine to combat MTB infection, allowing for more targeted drug delivery with enhanced efficiency and efficacy.

Acknowledgments

This project was supported by Researchers Supporting Project number (RSP2024R385), King Saud University, Riyadh, Saudi Arabia.

Conflict of interest

No potential conflict of interest was reported by the authors

Data availability statement





The datasets used and/or analyzed during the current study are available from the corresponding author on reasonable request.

References

- AHMAD, K.S., HAMID, A., NAWAZ, F., HAMEED, M., AHMAD, F., DENG, J., AKHTAR, N., WAZARAT, A., MAHROOF, S., 2017: Ethnopharmacological studies of indigenous plants in Kel village, Neelum Valley, Azad Kashmir, Pakistan. *J. Ethnobiol. Ethnomed.* 13(1), 1-16.
- AHMAD, S.A., DAS, S.S., KHATOON, A., ANSARI, M.T., AFZAL, M., HASNAIN, M.S., NAYAK, A.K., 2020: Bactericidal activity of silver nanoparticles: A mechanistic review. *Mat. Sci. Energy Technol.* 3, 756-769.
- ALVES, M.F., MURRAY, P.G., 2022: Biological synthesis of monodisperse uniform-size silver nanoparticles (AgNPs) by fungal cell-free extracts at elevated temperature and pH. *J. Fungi* 8(5), 439.
- BEZZA, F.A., TICHAPONDWA, S.M., CHIRWA, E.M., 2020: Synthesis of bio-surfactant stabilized silver nanoparticles, characterization and their potential application for bactericidal purposes. *J. Hazardous Materials* 393, 122319.
- DIEL, R., LODDENKEMPER, R., ZELLWEGER, J.P., SOTGIU, G., D'AMBROSIO, L., CENTIS, R., VAN DER WERF M.J., DARA, M., DETJEN, A., GONDRIE, P., REICHMAN, L., BLASI, F., MIGLIORI, G.B.; EUROPEAN FORUM FOR TB INNOVATION, 2013: Old ideas to innovate TB control: preventive treatment to achieve elimination. *Eur. Respir. J.* 42(3), 785-801. DOI: 10.1183/09031936.00205512
- DYE, C., SCHEELE, S., DOLIN, P., PATHANIA, V., RAVIGLIONE, M.C., 2013: Consensus statement. Global burden of tuberculosis: estimated incidence, prevalence, and mortality by country. WHO Global Surveillance and Monitoring Project. *JAMA* 282, 677-686.
- FARIQ, A., YASMIN, A., 2020: Production, characterization and bioactivities of biosurfactants from newly isolated strictly halophilic bacteria. *Process Biochemistry* 98, 1-10.
- FRAIMAN, D., FRAIMAN, R., 2018: An ANOVA approach for statistical comparisons of brain networks. *Scientific reports* 8(1), 4746.
- GHAFFARI-MOGHADDAM, M., HADI-DABANLOU, R., KHAJEH, M., RAKHSHANIPOUR, M., SHAMELI, K., 2014: Green synthesis of silver nanoparticles using plant extracts. *Korean J. Chem. Eng.* 31, 548-557. DOI: 10.1007/s11814-014-0014-6
- GLOBAL TUBERCULOSIS REPORT, 2020: Geneva: World Health Organization; 2020. IGO.
- HAQ, I., 2004: Safety of medicinal plants. *Pak. J. Med. Res.* 43(4), 203-210.
- HE JING, Z.C., 1978: *Flora China*, 74-75
- HE, M., REN, T., JIN, Z.D., DENG, L., LIU, H., CHENG, Y.Y., CHANG, H., 2023: Precise analysis of potassium isotopic composition in plant materials by multi-collector inductively coupled plasma mass spectrometry. *Spectrochim. Acta Part B: Atom Spectrosc.*, 106781. DOI: 10.1016/j.sab.2023.106781
- HUANG, B., GUI, M., AN, H., SHEN, J., YE, F., NI, Z., LIN, J., 2023: Babao Dan alleviates gut immune and microbiota disorders while impacting the TLR4/MyD88/NF-κB pathway to attenuate 5-Fluorouracil-induced intestinal injury. *Biomed. Pharmacother.* 166, 115387. DOI: 10.1016/j.biopha.2023.115387
- JAGTAP, U.B., BAPAT, V.A., 2013: Green Synthesis of Silver Nanoparticles Using *Artocarpus heterophyllus* Lam. Seed Extract and Its Antibacterial Activity. *Industr. Crop Prod.* 46, 132-137. DOI: 10.1016/j.indcrop.2013.01.019
- KASSAZA, K., ORIKIRIZA, P., LLOSA, A., BAZIRA, J., NYEHANGANE, D., PAGE, A.L., BOUM, Y., 2014: Lowenstein-Jensen selective medium for reducing contamination in *Mycobacterium tuberculosis* culture. *J. Clinical Microbiol.* 52(7), 2671-2673. DOI: 10.1128/JCM.00749-14
- KOWSHIK, M., ASHTAPUTRE, S., KHARRAZI, S., VOGEL, W., URBAN, J., KULKARNI, S.K., PAKNIKAR, K.M., 2003: Extracellular synthesis of silver nanoparticles by a silver-tolerant yeast strain MKY3. *Nanotechnology* 14(1), 95. DOI: 10.1088/0957-4484/14/1/321
- KREDY, H.M., 2018: The effect of pH, temperature on the green synthesis and biochemical activities of silver nanoparticles from *Lawsonia inermis* extract. *J. Pharmac. Sci. Res.* 10(8), 2022-2026. DOI: 10.1063/5.0129413
- KUMAR, V.V., ANTHONY, S.P., 2016: Antimicrobial studies of metal and metal oxide nanoparticles. In: *Surface chemistry of nanobiomaterials*, 265-300. William Andrew Publishing.
- LI, F., LI, D., LIU, H., CAO, B., JIANG, F., CHEN, D., LI, J., 2019: RNF216 Regulates the Migration of Immortalized GnRH Neurons by Suppressing Beclin1-Mediated Autophagy. *Front Endocrinol.* 10. DOI: 10.3389/fendo.2019.00012
- LIENHARDT, C., COOK, S.V., BURGOS, M., YORKE-EDWARDS, V., RIGOUTS, L., ANYO, G., KIM, S.J., JINDANI, A., ENARSON, D.A., NUNN, A.J., 2011: Efficacy and safety of a 4-drug fixed-dose combination regimen compared with separate drugs for treatment of pulmonary tuberculosis: the study C randomized controlled trial. *JAMA* 305, 1415-1423. DOI: 10.1001/jama.2011.436
- MARTINI, M.C., ZHANG, T., WILLIAMS, J.T., ABRAMOVITCH, R.B., WEATHERS, P.J., SHELL, S.S., 2020: *Artemisia annua* and *Artemisia afra* extracts exhibit strong bactericidal activity against *Mycobacterium tuberculosis*. *J. Ethnopharmacol.* 262, 113191. DOI: 10.1016/j.jep.2020.113191
- MAY, K., MARCHAND-AUSTIN, A., PECI, A., JAMIESON, F.B., 2019: A method for improved fluorescent staining for acid fast smear microscopy by incorporating an acetone rinse step. *Diagnostic Microbiol. Infect Disease* 93(4), 329-333. DOI: 10.1016/j.diagmicrobio.2018.11.002
- NATARAJAN, A., BEENA, P.M., DEVNIKAR, A.V., MALI, S., 2020: A systemic review on tuberculosis. *Indian J. Tuberculosis* 67(3), 295-311.
- PAL, S., TAK, Y.K., SONG, J.M., 2007: Does the antibacterial activity of silver nanoparticles depend on the shape of the nanoparticle? A study of the gram-negative bacterium *Escherichia coli*. *Appl. Environ. Microbiol.* 73(6), 1712-1720. DOI: 10.1128/AEM.02218-06

- PIRTARIGHAT, S., GHANNADNIA, M., BAGHSHAHI, S., 2019: Green synthesis of silver nanoparticles using the plant extract of *Salvia spinosa* grown in vitro and their antibacterial activity assessment. *J. Nanostruct. Chem.* 9, 1-9. DOI: [10.1007/s40097-018-0291-4](https://doi.org/10.1007/s40097-018-0291-4)
- RAI, M., YADAV, A., GADE, A., 2009: Silver nanoparticles as a new generation of antimicrobials. *Biotechnol. Advances* 27, 76-83. DOI: [10.1016/j.biotechadv.2008.09.002](https://doi.org/10.1016/j.biotechadv.2008.09.002)
- RAMAR, M., MANIKANDAN, B., MARIMUTHU, P.N., RAMAN, T., MAHALINGAM, A., SUBRAMANIAN, P., KARTHICK, S., MUNUSAMY, A., 2015: Synthesis of silver nanoparticles using *Solanum trilobatum* fruits extract and its antibacterial, cytotoxic activity against human breast cancer cell line MCF 7. *Spectrochimica Acta Part A: Mol. Biomol. Spectrosc.* 140, 223-228. DOI: [10.1016/j.saa.2014.12.060](https://doi.org/10.1016/j.saa.2014.12.060)
- ROY, K., SRIVASTWA, A.K., GHOSH, C.K., 2019: Anticoagulant, thrombolytic and antibacterial activities of *Euphorbia acruensis* latex-mediated bio-engineered silver nanoparticles. *Green processing and synthesis* 8(1), 590-599.
- SALEEM, S., JAFRI, L., UL HAQ, I., CHANG, L.C., CALDERWOOD, D., GREEN, B.D., MIRZA, B., 2014: Plants *Fagonia cretica* L. and *Hedera nepalensis* K. Koch contain natural compounds with potent dipeptidyl peptidase-4 (DPP-4) inhibitory activity. *J. Ethnopharmacol.* 156, 26-32. DOI: [10.1016/j.jep.2014.08.017](https://doi.org/10.1016/j.jep.2014.08.017)
- SASTRY, M., MAYYAA, K.S., BANDYOPADHYAY, K., 1997: pH dependent changes in the optical properties of carboxylic acid derivatized silver colloid particles. *Colloids Surfaces A: Physicochem. Eng. Asp.* 127, 221-228. DOI: [10.1016/S0927-7757\(97\)00087-3](https://doi.org/10.1016/S0927-7757(97)00087-3)
- SRIKAR, S.K., GIRI, D.D., PAL, D.B., MISHRA, P.K., UPADHYAY, S.N., 2016: Green synthesis of silver nanoparticles: a review. *Green Sustain Chem.* 6(1), 34-56.
- TAHSEEN, S., KHANZADA, F.M., BALOCH, A.Q., ABBAS, Q., BHUTTO, M.M., ALIZAI, A.W., ZAMAN, S., QASIM, Z., DURRANI, M.N., FAROUGH, M.K., AMBREEN, A., 2020: Extrapulmonary tuberculosis in Pakistan-A nationwide multicenter retrospective study. *PloS one* 15(4), p.e0232134. DOI: [10.1371/journal.pone.0232134](https://doi.org/10.1371/journal.pone.0232134)
- TANG, S., ZHENG, J., 2018: Antibacterial activity of silver nanoparticles: structural effects. *Adv. Healthcare Mat.* 7(13), 1701503. DOI: [10.1002/adhm.201701503](https://doi.org/10.1002/adhm.201701503)
- TUFAIL, M.S., LIAQAT, I., 2021: 2. Silver nanoparticles and their applications-A comprehensive review. *Pure Appl. Biol. (PAB)* 11(1), 315-330.
- VAZQUEZ-MUÑOZ, R., BORREGO, B., JUÁREZ-MORENO, K., GARCÍA-GARCÍA, M., MORALES, J.D.M., BOGDANCHIKOVA, N., HUERTA-SAQUERO, A., 2017: Toxicity of silver nanoparticles in biological systems: does the complexity of biological systems matter? *Toxicology letters* 276, 11-20.
- WHAYNE, T.F., 2018: Clinical Use of Digitalis: A State of the Art Review. *Am. J. Cardiovasc. Drugs* 18, 427-440.
- WHO, 2022: Catalysing Ancient Wisdom and Modern Science for the Health of People and the Planet. Available online: <https://www.who.int/initiatives/who-global-centre-for-traditional-medicine> (accessed on 3 August 2022).
- WHO, 2010: Treatment of tuberculosis: Guidelines for national programs, 4th ed. World Health Organization, Geneva.
- WHO/HTM/TB/2011.16. World Health Organization, 2014: Annual Report 2013. Retrieved from: <http://www.who.int/whr/en/>.
- WOODLEY, C.M., AMADO, P.S.M., CRISTIANO, M.L.S., O'NEILL, P.M., 2021: *Artemisinin* Inspired Synthetic Endoperoxide Drug Candidates: Design, Synthesis, and Mechanism of Action Studies. *Med. Res. Rev.* 41, 3062-3095. DOI: [10.1002/med.21849](https://doi.org/10.1002/med.21849)
- WORLD HEALTH ORGANIZATION, 2011: Global tuberculosis control. WHO report 2011.
- WORLD HEALTH ORGANIZATION, 2021: Global tuberculosis control. WHO report 2021.
- XIA, J., LI, Y., HE, C., YONG, C., WANG, L., FU, H., ZHANG, Y., 2023: Synthesis and Biological Activities of Oxazolidinone Pleuromutilin Derivatives as a Potent Anti-MRSA Agent. *ACS Infect Dis.* DOI: [10.1021/acsinfecdis.3c00162](https://doi.org/10.1021/acsinfecdis.3c00162)
- XIANG, J., MLAMBO, R., SHAW, I., SEID, Y., SHAH, H., HE, Y., HE, B., 2023: Cryopreservation of bioflavonoid-rich plant sources and bioflavonoid-microcapsules: emerging technologies for preserving bioactivity and enhancing nutraceutical applications. *Front Nutrition*, 10. DOI: [10.3389/fnut.2023.1232129](https://doi.org/10.3389/fnut.2023.1232129)
- XULU, J.H., NDONGWE, T., EZEALISIJ, K.M., TEMBU, V.J., MNCWANGI, N.P., WITIKA, B.A., SIWE-NOUNDOU, X., 2022: The Use of Medicinal Plant-Derived Metallic Nanoparticles in Theranostics. *Pharmaceutics* 14(11), 2437. DOI: [10.3390/pharmaceutics14112437](https://doi.org/10.3390/pharmaceutics14112437)
- YI, J., LI, L., YIN, Z., QUAN, Y., TAN, R., CHEN, S., ZHAO, J., 2023: Polypeptide from Moschus Suppresses Lipopolysaccharide-Induced Inflammation by Inhibiting NF- κ B-ROS/NLRP3 Pathway. *Chinese J. Integrat. Med.* 29, 895-904. DOI: [10.1007/s11655-023-3598-z](https://doi.org/10.1007/s11655-023-3598-z)
- YI, Z., YI, Z., HUANG, K., CAO, Y., XIAO, C., LI, Y., LIU, G., 2018: Propofol attenuates mast cell degranulation via inhibiting the miR-221/PI3K/Akt/Ca²⁺ pathway. *Exp. Ther. Med.* 16(2), 1426-1432. DOI: [10.3892/etm.2018.6317](https://doi.org/10.3892/etm.2018.6317)

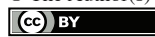
ORCID

- Suman Mahmood  <https://orcid.org/0000-0001-9107-4811>
- Sammyia Jannat  <https://orcid.org/0000-0001-8672-0655>
- Asad Hussain Shah  <https://orcid.org/0000-0002-5165-2864>
- Anila Fariq  <https://orcid.org/0000-0002-6016-5304>
- Sajida Rasheed  <https://orcid.org/0000-0002-6518-5136>
- Akhlaaq Wazeer  <https://orcid.org/0000-0002-7933-8914>
- Saleh H. Salmen  <https://orcid.org/0000-0002-2886-7998>
- Mohammad Javed Ansari  <https://orcid.org/0000-0002-8718-3078>
- Abdul Qayyum  <https://orcid.org/0000-0001-5322-7936>

Addresses of the corresponding authors:

- Sammyia Jannat, Department of Biotechnology, University of Kotli, 11100, Azad Kashmir, Pakistan
E-mail: sammyia@uokajk.edu.pk
- Abdul Qayyum, Department of Agronomy, The University of Haripur, Haripur 22620, Pakistan
E-mail: aqayyum@uoh.edu.pk

© The Author(s) 2024.

 This is an Open Access article distributed under the terms of the Creative Commons Attribution 4.0 International License (<https://creativecommons.org/licenses/by/4.0/deed.en>).